CRYSTAL GROWTH & DESIGN
2008
VOL. 8, NO. 2
507–511

Biogenic Guanine Crystals from the Skin of Fish May Be Designed to Enhance Light Reflectance

Avital Levy-Lior,[‡] Boaz Pokroy,[†] Berta Levavi-Sivan,[‡] Leslie Leiserowitz,[‡] Steve Weiner,[‡] and Lia Addadi[‡,*]

Departments of Structural Biology and Materials and Interfaces, Weizmann Institute of Science, Rehovot 76100, Israel, and the Department of Materials Engineering, Technion, Haifa, 32000, Israel, and the Department of Animal Sciences, Faculty of Agriculture, Hebrew University, Rehovot 76100, Israel

Received May 24, 2007; Revised Manuscript Received October 14, 2007

ABSTRACT: The metallic luster from the skin of fish is due to a photonic crystal system composed of multilayer stacks of cytoplasm and crystals. The crystals are described as thin (50−100 nm) plates of guanine, with no reference to their hydration state. We established through X-ray diffraction that their crystal structure is that of anhydrous guanine. We noted that their crystal structure-function relationship is exceptional compared to other purines with similar molecular stacking of the crystal structure. These elongate in the direction of molecular stacking, in contrast to the biogenic anhydrous guanine crystals whose smallest dimension is in the stacking direction. On the basis of the known crystal structure of anhydrous guanine, theoretical growth morphology was calculated. These calculations predict crystals elongated in the direction of the molecular stacking. The exposed molecular plane of the biogenic crystals is the (102) plane, which is composed of densely packed H-bonded guanine molecules. It is known that the in-plane polarizability of guanine molecules is significantly higher than the direction perpendicular to the molecular plane, most likely causing anisotropy of the crystals refractive index. It is therefore conceivable that the unique morphology observed in crystals from the skin of fish is designed to enhance their light reflective properties.

Introduction

The process of mineral formation in biological systems is termed biomineralization. Biomineralization is a diverse and widespread phenomenon. Organisms generally exhibit some degree of control over crystal nucleation and growth. The control over crystallization is expressed in the type of polymorph formed, crystal morphology, size, and orientation. It has been established that this control involves the interactions of specialized cellular membranes and/or macromolecular matrices, which delineate and control the microenvironment in which nucleation and growth occur, as well as biological macromolecules which directly interact with the growing crystals.[1] Although the term biomineralization refers to biogenic mineral formation, in practice, it includes within its scope organic crystal formation as well. These organic crystals fulfill functions similar to those of minerals.[1] Examples of biogenic organic crystals are oxalates, tartrates, and citrates found mainly in plants,[1–3] and purines such as uric acid and guanine, found in insects, reptiles, amphibians and fish.[4,5] Guanine is the most commonly formed purine.[4] Its presence in fish skin produces a metallic color and sometimes even iridescence.[6–8] These guanine crystals are the focus of this study.

Guanine is one of the five nucleic acid–bases and has the chemical formula $C_5H_5N_5O$. Guanine may crystallize as a monohydrate or in an anhydrous form. The crystal structure of the monohydrate[9] is monoclinic with the space group $P2_1/n$, and cell dimensions $a = 16.51$, $b = 11.28$, $c = 3.65$ Å, and $\beta = 96.8°$. The crystal structure of the anhydrous form has only recently been determined.[10] It is also monoclinic, with the space group $P2_1/c$ and cell dimensions $a = 3.55$,$b = 9.69$, $c = 16.35$ Å, and $\beta = 95.8°$. Both crystal structures have molecular arrangements involving stacking of the planar guanine molecules. This type of molecular packing is a very common feature of purine crystals.

Organic crystalline arrays found in the skin of many fish interact with incident light as photonic crystals to produce a mirror-like sheen.[6,11] Photonic crystals are periodic structures, with periodicities that affect the propagation of electromagnetic waves.[12] The use by animals of structures that produce metallic colors dates back as far as the Cambrian period[13,14] and is found in many living animals as well.[15–18]

In fish the metallic color is a result of constructive interference from multilayer arrays of crystals separated by cytoplasm.[6,11] The crystals are in the form of elongated semihexagonal thin plates in the range of 50−100 nm thick,[6,19] on average 20 μm long and 3 μm wide. Each crystal is enclosed within its own crystal chamber where crystallization most likely occurs.[4] These crystals have long been identified as guanine, although the reports have been unspecific as to the exact polymorph and crystal structure.[4,6,7,20–22]

Here we show that the guanine crystals found in the skin of many fish is in the form of anhydrous guanine and that their crystal structure is identical to the recently published structure.[10] We determined the morphology of anhydrous guanine crystals formed in vitro and biogenic anhydrous guanine crystals and show that the morphology differs from the theoretical form calculated from the known crystal structure. We suggest that control of crystal morphology is part of the strategy evolved by fish to produce more efficient photonic crystals.

Experimental Section

Materials. Biogenic crystals were extracted from the skin of the Japanese Koi fish (*Cyprinus carpio*) and Red-eye Tetra (*Moenkhausia sanctaefilomenae*of the family of *Characidae*). Anhydrous guanine was purchased from Sigma Aldrich (Lot 021K5008).

* To whom correspondence should be to addressed: E-mail: Lia.Addadi@weizmann.ac.il.
[†] Technion.
[‡] Weizmann Institute of Science.
[§] Hebrew University.

10.1021/cg0704753 CCC: $40.75
Published on Web 01/05/2008

Isolation of Biogenic Crystals. Fish scales were mechanically removed and washed in deionized water (DW). Crystals were extracted by placing the scales in a drop of DW, peeling the skin from the underside of the scale, and dispersing the crystals into the water. The crystal suspension was collected and centrifuged for 5−10 min at 10,600 rcf (Eppendorf centrifuge 5417C). The supernatant was replaced with DW, the pellet was resuspended, and the centrifugation was repeated twice.

Synthetic crystals of anhydrous guanine were grown in anhydrous dimethyl sulfoxide (DMSO). A saturated solution of guanine in DMSO was prepared and heated to 80 °C. The anhydrous guanine remnants were allowed to settle, the supernatant was transferred into a new vial and stored overnight at 4 °C. The crystal suspension was thawed at room temperature for 1 h then, centrifuged for 5 min at 1700 rcf. The supernatant was removed and replaced with absolute ethanol. The pellet was redispersed and centrifuged using the same conditions twice. The crystals were subsequently air-dried and stored at ambient temperature.

Conventional powder X-ray diffraction patterns of the biogenic crystals were obtained using a powder diffractometer (TTRAX III-Rigaku, Japan) with a Cu target attached to an UltraX rotating anode generator. The biogenic powder specimen was dispersed as a thin film on a Si zero-background holder and measured as is. Alternatively, a thin powder was prepared by crushing the biogenic crystals with a mortar and pestle before dispersing them on the holder.

The theoretical X-ray diffraction pattern of anhydrous guanine was generated using the known crystal structure of anhydrous guanine and the Cerius^2 program.

Synchrotron high-resolution powder diffraction measurements of the in vitro grown synthetic anhydrous guanine crystals were performed at the European Synchrotron Radiation Facility (ESRF, Grenoble, France) ID31 beamline, using synchrotron radiation, with $\lambda = 0.62$ Å at ambient temperatures. Crystals were crushed with a mortar and pestle. Powders were loaded into 1 mm diameter borosilicate glass capillaries. The capillaries were rotated during the measurements at a rate of 60 rps.

Pole-figures were measured in the Bragg–Brentano mode (Schultz method) on crystals supported on a Si zero-background holder on the powder diffractometer (TTRAX III-Rigaku, Japan). The reflections were recorded at a fixed Bragg angle while performing an in-plane rotation at regularly increasing sample tilt (90–50°) relative to the incident/diffracted beam plane.

Scanning electron microscopy (SEM) was performed with a LEO-Supra 55 VP FEG SEM (Zeiss). Samples were prepared by dispersing the crystals in either ethanol or DW. A drop of the crystal suspension was placed on a glass cover slide and was allowed to dry. It was then mounted on an aluminum SEM sample holder and coated with gold. In-situ samples were prepared by removing pieces of skin from a Red-eye Tetra fish (*Moenkhausia sanctaefilomenae*). These were fixed in 3% paraformaldehyde, 3% glutaraldehyde, and 0.1 Na cacodylate. Skin samples were dehydrated with ethanol and critical point dried (CPD). The samples were fractured to expose the cross-section, placed on a SEM aluminum sample holder, and sputter coated with gold. Gold sputtering was done on a S150 Sputter Coater (Edwards). Critical-point drying was performed using a CPD-030 (Bal-Tec).

Electron diffraction was performed using a T-12 (Technai-FEI) transmission electron microscope (TEM) operated at 120 kV. Samples were prepared by placing a drop of the crystal suspension on a copper carbon-coated TEM grid, allowing the crystals to settle for 30 s and then removing the remaining suspension.

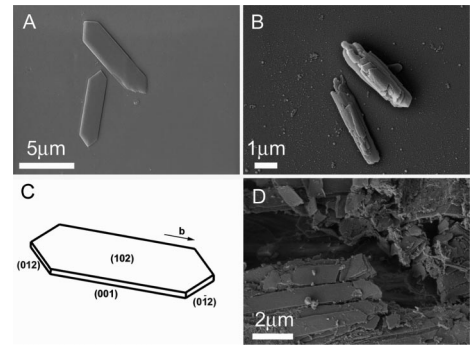

Figure 1. (A) SEM micrographs of isolated biogenic crystals from the skin of Japanese Koi fish. The crystals adopt elongated semihexagonal platelike forms. (B) SEM micrograph of in vitro grown anhydrous guanine crystals crystallized from an anhydrous solution of DMSO. They are stepped and much thicker than the biogenic form. (C) Schematic representation of the morphology of the biogenic crystals. The crystal planes identified are the (102) basal plane and the {001} and {012} planes. (D) Guanine platelets from fish skin. The multiple layer assembly of the single crystals is observed in situ.

Theoretical morphology prediction calculations were performed applying three different force fields, Dreiding II, CVFF, and COMPASS, to the crystal structure of anhydrous guanine. The growth morphology was calculated using the Attachment Energy[23] (AE) Cerius^2 (Accelrys) morphology prediction module, after energy minimization and optimization of the crystal structure.

Results

Biogenic guanine crystals were collected from the skin beneath the scales of Koi fish (*Cyprinus carpio*) and in vitro guanine crystals were grown from anhydrous DMSO. Although crystals show resemblance in form (Figure 1A and B), the biogenic crystals are exceptionally thin (∼50 nm) with well-defined crystal faces while the crystals grown in vitro are much thicker and irregularly stepped. Here, we characterized the detailed morphologies of the crystals relative to the structure using X-ray and electron diffraction, as well as transmission electron microscopy (TEM) and scanning electron microscopy (SEM).

X-ray Powder Diffraction. X-ray powder diffraction data were collected at ambient temperature from thin films of biogenic crystals (Figure 2A), as well as from crushed biogenic crystals (Figure 2B). The diffraction pattern from the uncrushed crystals has only four strong reflections, implying that the crystals have a well-defined preferred orientation in or close to the (102) plane. This is not surprising because of their platelike morphology. When dispersed, most of the biogenic crystals are expected to be oriented such that they lie on their large basal planes. The peaks measured correspond to *d*-spacings of 3.21, 3.03, 1.61, and 1.07 Å, respectively. A pole-figure measurement was conducted on these crystals at a constant 2θ angle corresponding to that measured for the (102) plane (Figure 2E). The (102) plane can be detected up to a 10° incline of the specimen, indicating that the crystals are orientated such that their basal plane is the (102) crystal plane.

The diffraction pattern from the crushed biogenic crystals also shows a preferred orientation (Figure 2B) of the (102) family of planes and other closely related planes. The X-ray powder

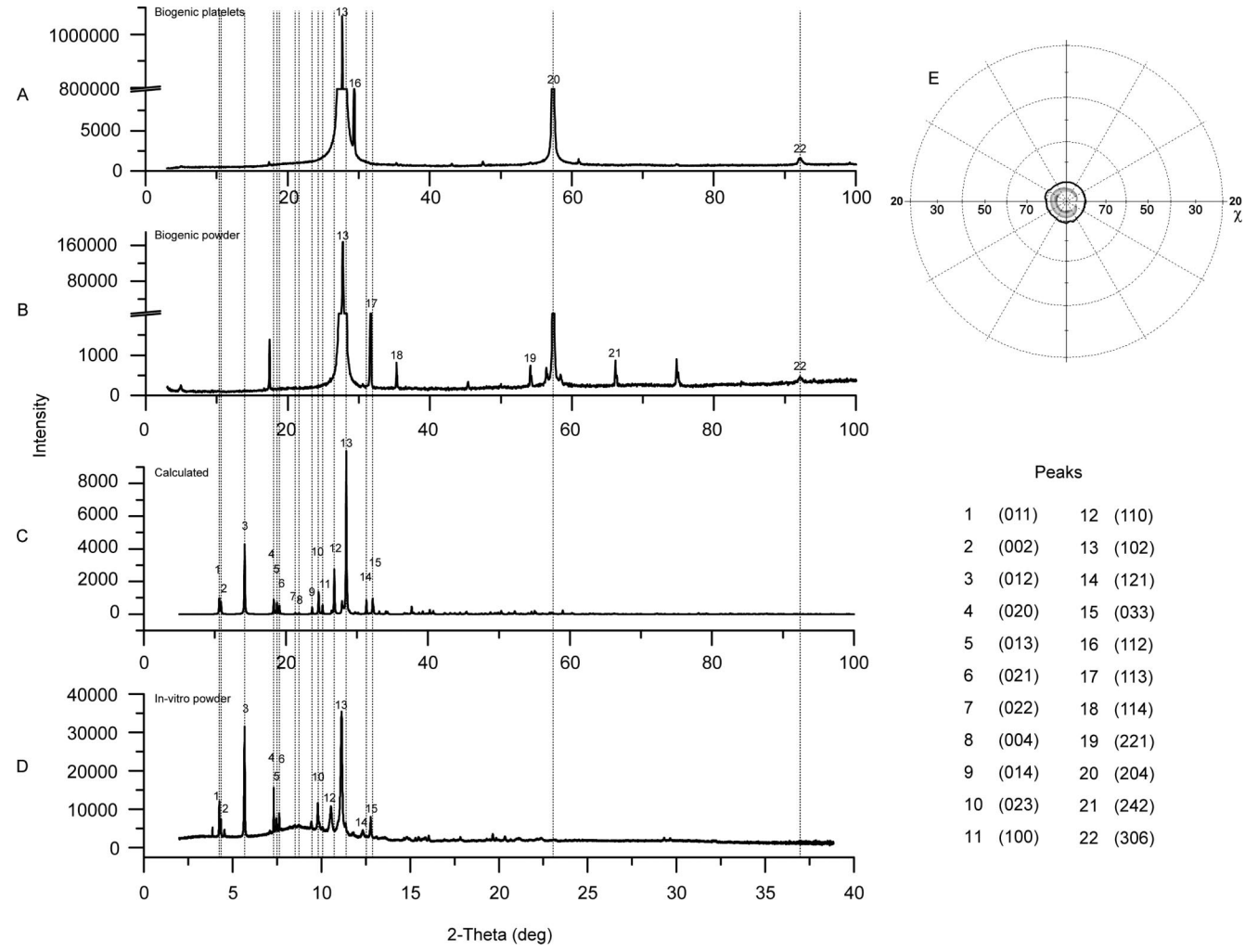

Figure 2. (A) X-ray powder diffraction patterns of biogenic crystals collected from fish skin. Reflections of the (102), (204), and the (306) planes are observed and correspond to the *d*-spacings: 3.22, 3.04, 1.61, and 1.07 Å. The spectra indicate a strong preferred orientation of the crystals. $\lambda = 1.54$ Å. (B) Crushed biogenic crystals collected from fish skin. These still produce a pattern with a strong preferred orientation. $\lambda = 1.54$ Å. (C) X-ray diffraction pattern calculated from the known crystal structure of anhydrous guanine.[10] (D) Synchrotron X-ray diffraction pattern of anhydrous guanine crystals grown in vitro. There is observed intensity enhancement of the peaks corresponding to the (012), (020), (013), and (021) planes relative to the (102). This was not observed in the diffraction of the biogenic crystals, indicating a different preferred orientation of these crystals compared to the biogenic crystals. $\lambda = 0.62$ Å. (E) Pole-figure plot of the (102) crystal plane. The diffraction angle 2θ was held constant at 27.7° while the sample orientation angle was (χ) changed between 90° and 50°. This shows that the biogenic crystals lie preferentially on their (102) plane.

diffraction pattern calculated from the published anhydrous guanine crystal structure (measured at a temperature of 120 K)[10] is shown in Figure 2C. All the peaks are slightly shifted relative to those of the biogenic crystals. Multiplying the *d*-spacing values of the experimental data by a constant factor of 0.973 eliminates this small shift. This factor is most likely due to the difference in temperature between the measurements.

X-ray powder diffraction patterns were collected from in vitro grown crystals of anhydrous guanine using synchrotron radiation (wavelength 0.62Å) (Figure 2D). The *d*-spacings calculated from the measured diffraction peaks are shifted by a factor of 0.991 relative to the peaks calculated from the anhydrous guanine crystal structure. A number of peaks appear that are not related to the crystal structure. These are believed to be due to contamination of the original material. The pattern fits that of the crystal structure determined for the anhydrous guanine.[10] Note that in contrast to the biogenic crystals, in the X-ray diffraction spectra of the in vitro grown crystals the intensities of the peaks corresponding to the (012), (020), (013), and (021) planes are enhanced relative to the (102) peak. This indicates a different preferred orientation of these crystals relative to the biogenic crystals. This may be due to different crystal morphologies or to a preferential cleavage along these planes.

Electron Microscopy. Scanning and transmission electron microscopy (SEM and TEM) were used to study biogenic and in vitro grown anhydrous guanine crystals. Isolated biogenic crystals from the scales of fish have an elongated hexagonal platelike form[6] (Figure 1A). The morphology of the crystals was determined by examining crystals lying on the (102) basal plane, as identified by X-ray diffraction. The crystal habit was determined by measuring the dihedral angles between the adjoining crystal faces of the plates. These can be observed nearly edge-on in the plates lying on their basal plane. The measured dihedral angles were found to be 134.2 ± 3° and 91.6 ± 3°. The morphology was reconstructed by fitting the dihedral angle measurements to the known crystal structure.[10] The crystal planes, in addition to the (102) basal plane, were identified as {001} and {012} (or {023}) (Figure 1B), which form calculated dihedral angles of 140° and 100°. In situ, these crystals are observed to be assembled in a multilayered organization (Figure 1C). In-vitro grown anhydrous guanine crystals crystallized from

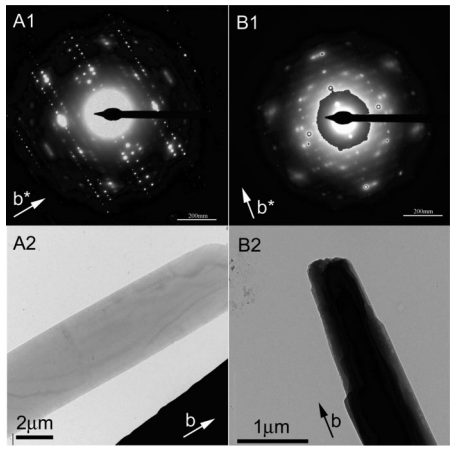

Figure 3. Electron diffraction patterns (A1 and B1) and TEM micrographs (A2 and B2) of (A) a biogenic guanine crystal and (B) an in-vitro grown anhydrous guanine crystal. The two diffraction patterns are essentially the same and correspond to the [100] zone axis of anhydrous guanine.

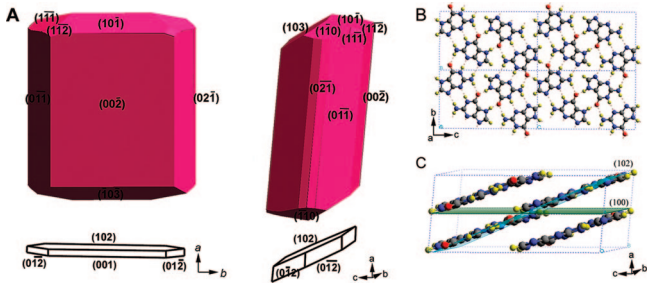

Figure 4. (A) Theoretical growth morphology of anhydrous guanine, calculated using the Dreiding II force field (top, pink) and morphology of biogenic crystals (bottom, white); (left) projection approximately on the (*a,b*) plane; (right) projection approximately on the (*a,c*) plane. (B) Crystal structure of anhydrous guanine in the (102) plane, displaying the H-bonding network. (C) Crystal structure of anhydrous guanine in the (010) plane, showing the molecular stacking of the planar guanine molecules: (gray) carbon, (blue) nitrogen, (yellow) hydrogen, (red) oxygen.

anhydrous DMSO have morphologies similar to those of the biogenic crystals but are much thicker and irregular (Figure 1D).

Electron diffraction patterns of biogenic crystals and in vitro grown anhydrous guanine crystals were acquired without tilting the stage or adjustment of the specimens (Figures 3 and 4). The symmetry of the reciprocal cell dimensions of the biogenic (Figure 4A) and synthetic (Figure 4B) crystal electron diffraction patterns are almost identical. From these diffraction patterns, two principle spacings of length 9.4 and 17.7 Å are calculated, forming an angle of 90°.

When compared to the diffraction patterns expected from the crystal structure of anhydrous guanine, the zone axis was identified as [100]. In agreement with the space-group $P2_1/c$, the (0*kl*) electron diffraction pattern (Figure 3; A1, B1) shows no general systematic absences, but for the systematic absences along the *b** and *c** axes (reflections (0*k*0) and (00*l*) absent for *k* and *l* odd). The observed [100] zone axis is surprising since from X-ray diffraction it was established that the crystal plates lie on the (102) basal plane. On the other hand, the diffraction pattern for the (102) zone axis should consist of a pattern of only two diffraction spots from the {020} family of planes. Some electron diffraction patterns of this kind were indeed observed, although most corresponded to the [100] zone axis.

Theoretical morphology. In order to avoid model-dependent artifacts, theoretical morphology prediction calculations were performed applying three different force fields: Dreiding II (Figure 4A, top), CVFF (Figure S1A in the Supporting Information), and COMPASS (Figure S1B in the Supporting Information). The growth morphology was then calculated using the Attachment Energy[23] (AE) model. The Dreiding II force field results in the best fit between the optimized and measured crystal structure; in addition, it is the only one which relates explicitly to hydrogen bonding. In contrast, the theoretical morphology generated using CVFF and COMPASS force fields caused a distortion of the crystal structure during the geometrical optimization. As might be intuitively expected from consideration of the crystal packing (Figure 4B and C), all three predicted morphologies are prismatic, with *a* (the direction of molecular stacking) as the prism height. Application of the CVFF force field yields prisms with an aspect ratio *a*/*b* of ∼1.1, COMPASS results in an aspect ratio *a*/*b* = ∼1.5, while Dreiding is intermediate between the previous two, with an aspect ratio *a*/*b* = ∼1.2. All three force fields are in good agreement with the predicted growth direction and morphology and differ mainly in the developed faces terminating the crystal along the *a* axis and in the crystal aspect ratio.

The theoretical morphology thus differs drastically from the morphology of the biogenic anhydrous guanine crystals, i.e., thin plates with aspect ratio *a*/*b* = ∼0.05 (Figure 4A, bottom). The biogenic plates develop in directions perpendicular to the stacking direction *a*, i.e. parallel to the hydrogen-bonded network, and are elongated along *b* (Figure 4B and C).

Discussion

The structure of biogenic crystals from the skin of the Japanese Koi fish was established through X-ray powder diffraction data as being identical to that of the published structure of anhydrous guanine.[10] The biogenic crystals are thin plates with the main developed face parallel to the {102} plane. This was unequivocally established from the pole-figure measurement. This result is consistent with the X-ray powder diffraction data in which the higher order reflections of the {102} are strongly observed ({204} and {306}) as a result of preferred crystal orientation, in the diffraction measurements. This persists even after the biogenic crystals were crushed. In contrast, the in-vitro grown crystals of anhydrous guanine are much thicker and irregular in shape (Figure 1D). The powder diffraction pattern of these crystals, when crushed, showed intensity enhancement of the {0*kl*} reflections relative to the (102) plane, indicating that the crushed synthetic crystals have a different morphological anisotropy from the biogenic crystals.

The single crystal electron diffraction patterns obtained from the [100] zone axis suggests that the plate face is of the type {100}, because the angle between the zone axis [100] and *a** is only 5.8° (i.e., $\beta - 90°$). However, this interpretation is inconsistent with the fact the crystal plates have the form {102}, as determined from the pole-figures. The angle between the *a* axis and the [102] reciprocal vector is 28°. We suggest that because the biogenic crystals are elongated in the direction of the *b* axis, the crystals dispersed on the electron microscope grid frequently tilt about this direction. This allows the richer diffraction pattern from the [100] zone axis to be readily observed, rather than the two {020} reflections that would be observed had the reciprocal vector *d**(102) been parallel to the electron beam. This poor diffraction pattern was nevertheless observed, although less frequently than the {0*kl*} diffraction pattern.

Crystal morphology is defined by the relative rate of its growth in different directions.[24] In other words, the size of a crystal face is inversely proportional to the rate of crystal growth perpendicular to the face. Rate of growth is determined by an interplay between various contributions, i.e. that of the internal crystal structure and external influences provided by the environment of the crystal. The anhydrous guanine crystal structure exhibits a molecular stacking arrangement of the planar guanine molecules in the direction of the short crystallographic axis ($a = 3.553$). This characteristic stacking arrangement is observed in other purines such as guanine monohydrate, allopurinol, sodium urate, inosine, and purine. These crystals have a characteristic morphology elongated along their short crystal axis (i.e., in the direction of the stacking).[9,25–28]

The theoretical growth morphology calculated for anhydrous guanine using three different force fields is consistent with the crystal structure-morphology relationships described for other purines. It is thus most surprising that the crystal morphology of the biogenic guanine crystals is so drastically different from the calculated theoretical morphology. The biogenic crystals are very thin plates, with the shortest dimension of the crystals in the direction that would be expected to exhibit the highest growth rate. The interplay between the layer energy and attachment energy would have to change dramatically in order to introduce an orthogonal change in habit. It is thus concluded that growth of the biogenic crystals must be strongly inhibited along this direction of natural crystal growth to produce such an unexpected morphology.

The synthetic crystals of anhydrous guanine resemble the morphology of the biogenic crystals in that they too are inhibited in the stacking direction, possibly by interference of the DMSO solvent with the guanine stacking. When the DMSO solution is not completely dry, the anhydrous guanine crystals simply do not form. The dry environment is therefore believed to be necessary for the crystallization of anhydrous guanine. It is known that each biogenic crystal forms within its own crystal chamber.[4] It is therefore conceivable that the delimited compartment contains very little, if any, bulk water allowing the formation of the anhydrous form of guanine. In addition, the fish have developed an incredibly efficient mechanism that inhibits growth in the stacking direction. How this might occur is still not understood.

A multilayer reflector system is characterized by the optical thickness of its constituents, i.e. their refractive indices and the thickness of the layers. The fish form photonic crystals that are multilayered arrays of two media with different optical properties: the guanine crystals are the medium with the higher refractive index, and the cytoplasm is the medium with the lower refractive index.

The crystal morphology that the fish evolved and its relation to the crystal structure may be significant in terms of the reflective properties of the crystal arrays. Fish have evolved a mechanism to efficiently inhibit crystal growth in the direction of the molecular stacking. This results in thin crystal plates of guanine, orientated such that the main developed crystal face exposed to the light is the planar H-bonded network of guanine molecules. It is known that the molecular polarizability of guanine molecules is significantly higher in-plane than in the direction perpendicular to the molecule.[29] Thus, birefringence of the guanine crystals is expected and it is conceivable that the refractive index of the (102) crystal face is significantly higher than in the direction perpendicular to this face. The molecular flatness of this layer also enhances light reflectivity. These may be the reasons why fish invest energy in inhibiting crystal growth in the fast growing direction. In this way, they form crystals with the best possible optical properties for reflection.

Acknowledgment. We thank Talmon Arad, Yishay Feldman, Carlota Conesa-Moratilla, Michela Brunelli, and Emil Zolotoyabko for their help in furthering this work. We thank ESRF for beamtime. L.A. is the incumbent of the Dorothy-and-Patrick-Gorman Professorial Chair of Biological Ultrastructure, and S.W is the incumbent of the Dr. Walter and Dr. Trude Burchardt Professorial Chair of Structural Biology.

Supporting Information Available: Predicted morphology using the Attachment Energy module in the Cerius^2 program and applying the CVFF force field and predicted morphology using the Attachment Energy module in the Cerius^2 program and applying the compass force field. This material is available free of charge via the Internet at http://pubs.acs.org.

References

(1) Lowenstam, H. A.; Weiner, S. In *On Biomineralization*; Oxford University Press: New York, 1989.
(2) Franceschi, V. R.; Horner, H. T. *Bot. Rev.* **1980**, 361–427.
(3) Arnott, H. J.; Pautard, F. G. E. In *Biological Calcification*; Schraer, H., Ed.; Appleton-Century Crafts: 1970; p 375.
(4) Fox, D. L. In *Animals Biochromes and Structural Colours*; Cambridge University Press: Cambridge, 1953.
(5) Millot, J. *Bull. Biol. France Belgique.* **1923**, 261–363.
(6) Denton, E. J. *Phil. Trans. R. Soc. Lond., B* **1970**, *258*, 285–313.
(7) Cunningham, J. T.; MacMunn, C. A. *Phil. Trans. R. Soc. Lond., B* **1893**, *184*, 765–812.
(8) Mathger, L. M.; Land, M. F.; Siebeck, U. E.; Marshall, N. J. *J. Exp. Biol.* **2003**, *206*, 3607–3613.
(9) Thewalt, U.; Bugg, C. E.; Marsh, R. E. *Acta. Crystallogr. B* **1971**, *B27*, 2358–2363.
(10) Guille, K.; Clegg, W. *Acta. Crystallogr. C* **2006**, *62*, O515–O517.
(11) Arnott, H. J.; Nicol, J. A. C. *Can. J. Zool.* **1970**, *48*, 137–151.
(12) Joannopoulos, J. D.; Robert, D. M.; Joshua, N. W. In *Photonic Crystals - Molding the Flow of Light*; University Press: Princeton, 1995.
(13) Parker, A. R. *Proc. R. Soc. Lond., B* **1998**, *265*, 967–972.
(14) Parker, A. R. *J. Opt. A: Pure Appl. Opt.* **2000**, *2*, R15–R28.
(15) Vukusic, P.; Sambles, J. R.; Lawrence, C. R.; Wootton, R. J. *Proc. R. Soc. Lond., B* **1999**, *266*, 1403–1411.
(16) Parker, A. R.; McKenzie, D. R.; Large, M. C. J. *J. Exp. Biol.* **1998**, *201*, 1307–1313.
(17) Mason, C. W. *J. Phys. Chem.* **1926**, *31*, 321–354.
(18) Land, M. F. *J. Opt. A: Pure Appl. Opt.* **2000**, *2*, R44–R50.
(19) Kawaguti, S. *Proc. Jpn. Acad.* **1965**, *41*, 610–613.
(20) Harmer, S. C.; Shipley, A. E. In *Fish and Ascidians etc.*; Macmillon and Co.: New York, 1910.
(21) Nakata, A. *J. Shimonoseki Coll. Fish* **1955**, *5*, 113–115.
(22) Barraud, J.; Bassot, J. M.; Favard, P.; Jean, W. *Acad. Sci.* **1959**, 2633–2637.
(23) Berkovitch-Yellin, Z.; Vanmil, J.; Addadi, L.; Idelson, M.; Lahav, M.; Leiserowitz, L. *J. Am. Chem. Soc.* **1985**, *107*, 3111–3122.
(24) Hartman, P.; Perdok, W. G. *Acta. Crystallogr. A* **1955**, *8*, 49–52.
(25) Watson, D. G.; Sweet, R. M.; Marsh, R. E. *Acta Crystallogr.* **1965**, *19*, 573–580.
(26) Prusiner, P.; Sundaral, M. *Acta. Crystallogr. B* **1972**, *B 28*, 2148–2152.
(27) Rinaudo, C.; Boistelle, R. *J. Cryst. Growth* **1982**, *57*, 432–442.
(28) Chiarella, R. A.; Gillon, A. L.; Burton, R. C.; Davey, R. J.; Sadiq, G.; Auffret, A.; Cioffi, M.; Hunter, C. A. *Faraday Discuss.* **2007**, *136*, 179−193.
(29) Clark, L. B. *J. Am. Chem. Soc.* **1994**, *116*, 5265–5270.

CG0704753